

Numerical Modeling of Inflatable Cylinder

Bhaveshkumar N. Pasi, Vaibhav Pawar, Ameya J. More

Abstract—Inflatable materials find a wide range of applications in structural field as they are light, strong, anti-corrosive and can be moulded in any shape. Due to its advantage of light weightiness and ease of transportability, inflatable has been the area of research since our past and more over it has been attracted even today's genesis toward itself in its commercial application, civilian applications as well as in defence too. This paper focuses on determination of deformation and stresses for inflatable cylinder under various conditions by using ANSYS 14.5.

Index Terms—Deflection, Inflatable Cylinder, Inflatable Material, Stresses.

I. INTRODUCTION

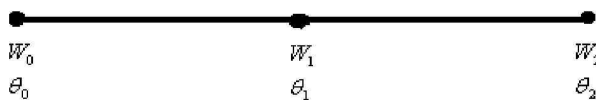
Ongoing researches in inflatable science have increased their uses in manufacturing of inflatable castles, inflatable boat, inflatable balloon, etc. Till today's date, the stresses of the inflatable beam are modeled mathematically and the general expressions of the same are listed out. The model is based on the boundary conditions chosen pertaining to the application of project in mind. Deflection and stress of the beam are also found out mathematically and the equations are derived.

II. MATHEMATICAL MODELING

A. Stiffness Matrix and Deflection

Let us consider an inflatable cylinder of length l , radius R , area of cross section S , moment of Inertia I , Young's Modulus E , Shear Modulus G and Shear Coefficient k . According to J.C. Thomas et al., we obtain the stiffness matrix of the inflatable cylinder which is as shown below

$$K = \frac{EI + \frac{PI}{S}}{l^3(1 + \phi_p)} \begin{bmatrix} 12 & \mathcal{A} & -12 & \mathcal{A} \\ \mathcal{A} & l^2(4 + \phi_p) & -\mathcal{A} & l^2(2 - \phi_p) \\ -12 & -\mathcal{A} & 12 & -\mathcal{A} \\ \mathcal{A} & l^2(2 - \phi_p) & -\mathcal{A} & l^2(4 + \phi_p) \end{bmatrix}$$



$$[K][U] = [F]$$

B. Stresses in Inflatable Cylinder

The beam is anisotropic with vertical Young's Modulus = E and horizontal young's modulus as E/m where m is the anisotropic ratio. The Poisson's ratio expressing a horizontal strain due to vertical stress is μ . Poisson's ratio expressing a

vertical strain due to horizontal stress is μ/m , W is the externally applied load and P is the internal pressure.

$$\frac{EI + \frac{PI}{S}}{l^3(1 + \phi_p)} \begin{bmatrix} 12 & 3L & -12 & 3L & 0 & 0 \\ 3L & \frac{E}{4}(4 + \phi_p) & -3L & \frac{E}{4}(2 - \phi_p) & 0 & 0 \\ -12 & -3L & 24 & 0 & -12 & 3L \\ 3L & \frac{E}{4}(2 - \phi_p) & 6L & \frac{E}{2}(4 + \phi_p) & -3L & \frac{E}{4}(2 - \phi_p) \\ 0 & 0 & -12 & -3L & 12 & -3L \\ 0 & 0 & 3L & \frac{E}{4}(2 - \phi_p) & -3L & \frac{E}{4}(4 + \phi_p) \end{bmatrix} \begin{bmatrix} W_0 \\ \theta_0 \\ W_1 \\ \theta_1 \\ W_2 \\ \theta_2 \end{bmatrix} = \begin{bmatrix} -PL/4 \\ -PE/48 \\ -PL/2 \\ 0 \\ -PL/4 \\ PE/48 \end{bmatrix}$$

$$\frac{EI + \frac{PI}{S}}{\frac{E}{8}(1 + \phi_p)} \begin{bmatrix} 24 & 0 & -12 \\ 6L & \frac{L^2}{2}(4 + \phi_p) & -3L \\ -12 & -3L & 12 \end{bmatrix} \begin{bmatrix} W_1 \\ \theta_1 \\ W_2 \end{bmatrix} = \begin{bmatrix} -PL/2 \\ 0 \\ -PL/4 \end{bmatrix}$$

Where,

$$\phi_p = \frac{12 \left(EI + \frac{PI}{S} \right)}{(P + KGS) L^2}$$

III. NUMERICAL ANALYSIS

A. Element Selection and Modeling

The geometry of the profile is created using key points which are marked which constitute for the first half of the cylinder profile. Using the 'Extrude' option, the straight line is revolved around its axis along 360 degrees; we obtain the hollow cylinder which is of negligible thickness. The geometry is created and the cylinder area is meshed with rectangular shell elements. The material is modeled as a thin fabric by specifying the fabric thickness accordingly.

Since the fabrics exhibit tensile stiffness and not a considerable deal of compressive stiffness, a thin shell element with optional compressive stiffness is suitable. Shell 181 element is apt for such an application. The deflection and the stress patterns derived from the run from SHELL 181 found acceptable patterns which could be related to the theoretical results. The values of the elastic moduli and shear moduli are obtained from pre-done experimental analysis which can be used as references. However, the Poisson's ratio can be chosen based on finite element analysis results.

B. Boundary Condition

In any finite element analysis, the accuracy of the result is governed by the type of boundary condition considered. For our application, as we can see in the fig. 1 below, the cylinder is stationed on a hinge on one side and is simply supported at the other with central point load acting on the top surface. In order to emulate this in FEM, one end of the cylinder is completely constrained with resistance along UX and UY fully along the circumference which would represent the simply supported end, and the other end is completely constrained with resistance along UX and UY along the entire circumference except the two nodes diametrically opposite at the horizontal centre of the cylinder. These two nodes are constrained with resistance along UX, UY and UZ

Revised Version Manuscript Received on May 18, 2015.

Bhaveshkumar N. Pasi, Mechanical Engineering Department, Pillai HOC College of Engineering and Technology, Mumbai, India.

Vaibhav Pawar, Asst. Prof, Mechanical Engineering Department, Pillai HOC College of Engineering and Technology, Rasayani, Panvel, India.

Ameya J. More, Asst. Prof, Mechanical Engineering Department, Pillai HOC College of Engineering and Technology, Rasayani, Panvel, India.

which signifies that the movement is arrested, thus behaving like a hinged cylinder.

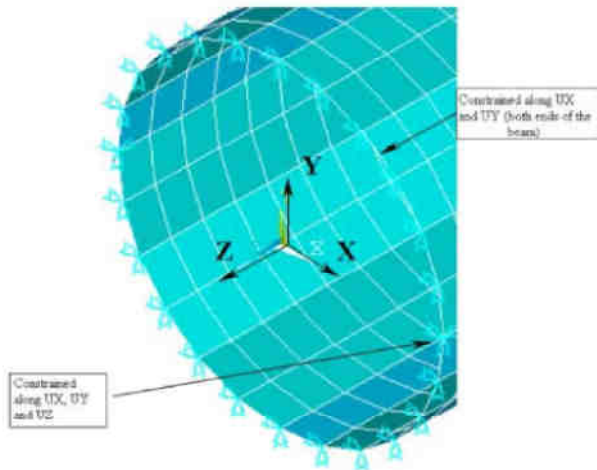


Figure 1: Boundary Conditions

IV. VARIOUS CASES TO BE ANALYZED

A. Case I: Thin walled cylinder is pinched by F at the middle of cylinder length. The ends of the cylinder are free edges. (Static linear analysis)

Table 1: Parameters Used in Modeling

Material Properties	Geometric Properties	Loading
$E = 10.5 \times 10^6$ psi $\nu = 0.3125$	$l = 10.35$ in $r = 4.953$ in $t = 0.094$ in	$F = 100$ lb

Meshing:

Fig. 2 below shows the meshed model. Rectangular meshing is used for verification model.

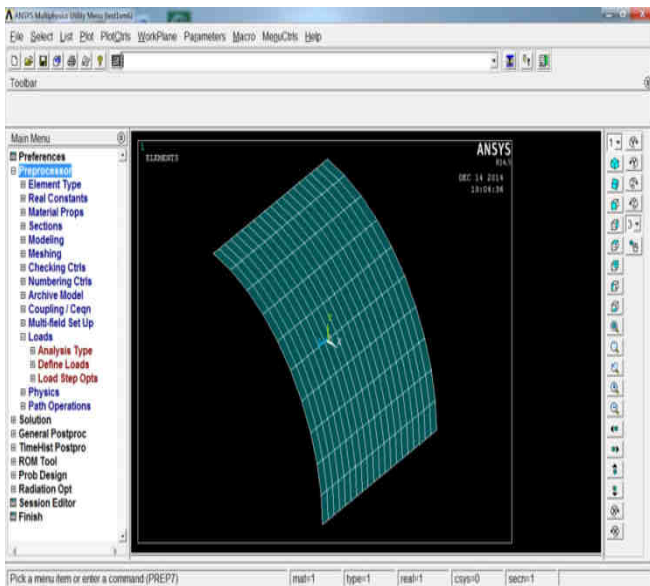


Figure 2: Meshed Model

Results and Discussion:

Fig. 3 shows the displacement of inflatable tube model when load is applied centre of span. The maximum deflection value is 0.100254 in. ANSYS value is matched closely with target value. Small variation is observed in ANSYS result due to round off error.

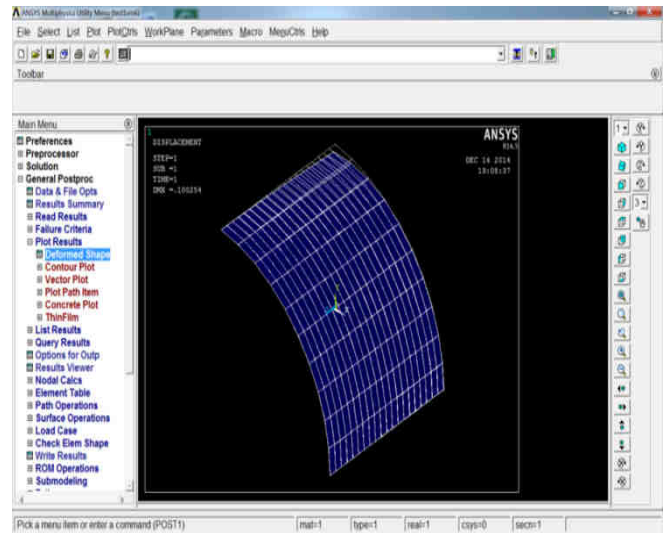


Figure 3: Deflection Due to Point Load at Mid Span

B. Case II: A cylindrical membrane container of diameter ' d ' and wall thickness ' t ' is subjected to a uniform internal pressure ' P '. (Static non-linear analysis)

Table 2:- Parameters Used in Modeling

Material Properties	Geometric Properties	Loading	Bilinear Isotropic Hardening
$E = 30 \times 10^6$ psi $\nu = 0.3$	$t = 1$ in $r = 120$ in	$P = 500$ psi	Yield Stress = 250 Tang Mod = 2000

Meshing:

Fig. 4 shows the meshed model. Rectangular meshing is used for verification model.

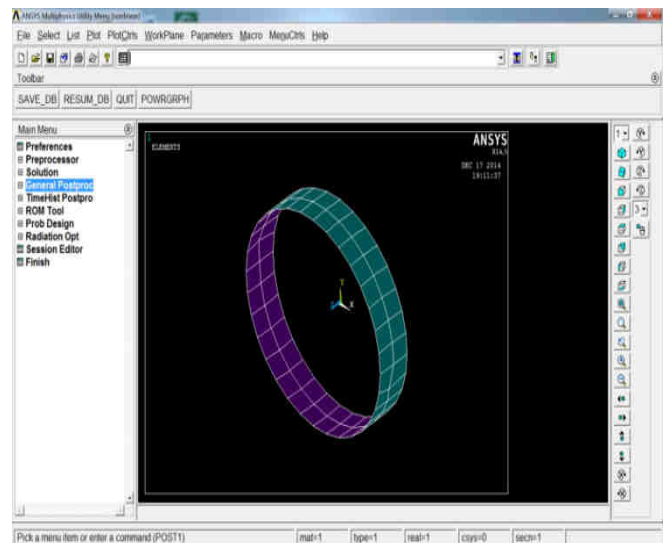


Figure 4: Meshing

Results and Discussion:

Fig. 5 shows the stress of inflatable cylinder model when internal pressure is applied. The maximum stress value is 328.956. ANSYS value is matched closely with target value.

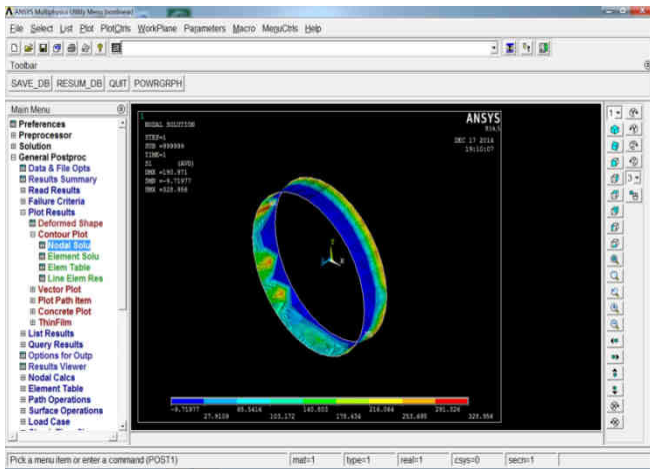


Figure 5: Stress

C. Case III: A cylindrical membrane container of diameter 'd' and wall thickness 't' is subjected to a uniform internal pressure 'P' and external atmospheric pressure.

Meshing:

In ANSYS 14.5 automatic meshing is done. For the given model as shown in fig. 6 automatic meshing is performed.

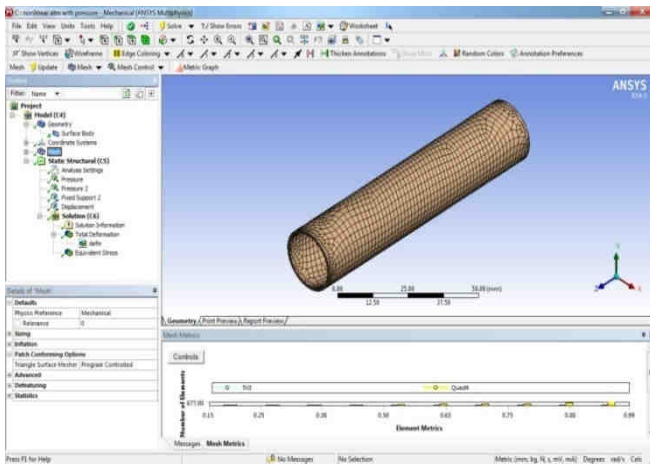


Figure 6: Meshing

Boundary Conditions:

Accuracy of results depends upon boundary conditions. Hence, boundary conditions must given with great care. As shown in fig. 7, tube is subjected to an internal pressure of 0.12 MPa and external pressure of 0.1 MPa.

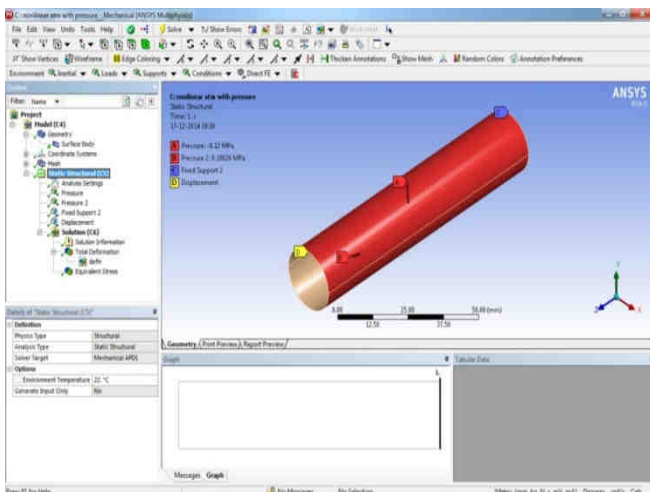


Figure 7: Boundary Condition

Results and Discussion:

A. Stress:

Maximum value of equivalent stress is 12.173 MPa. Standard available result for this case is 11.23 MPa. Small variation in result is obtained due to round off error.

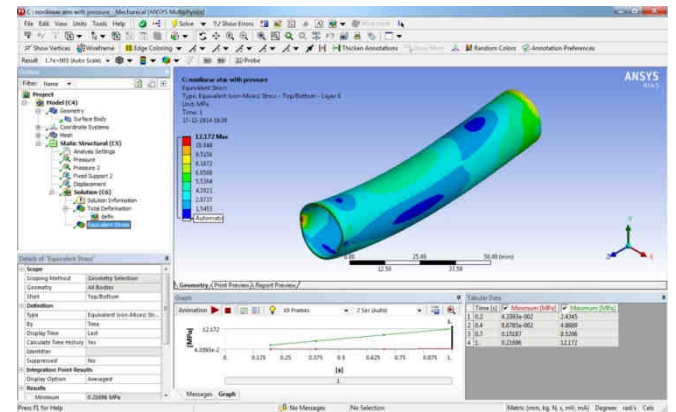


Figure 8: Stress

B. Deformation:

Maximum value of deformation is 0.003017 mm. Standard available result for this case is 0.00298 mm. Small variation in result is obtained due to round off error.

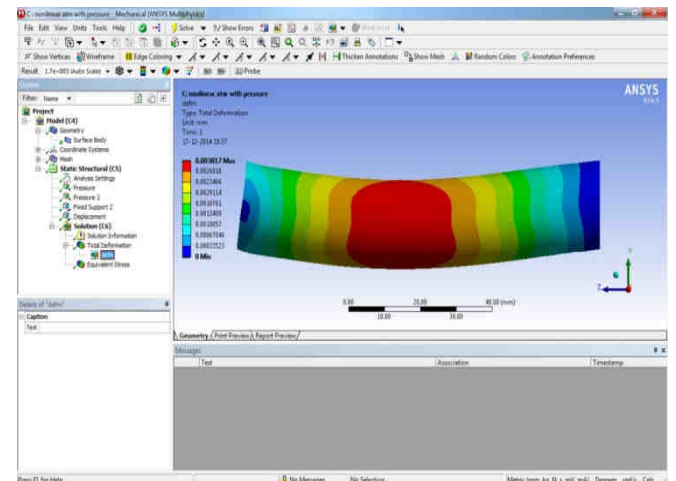


Figure 9: Deformation

V. RESULT COMPARISON

Table III: Result Comparison

Cases	Parameters	Target	ANSYS
Case I	Deflection (inch)	0.1139	0.100254
Case II	Stress (MPa)	330.96	328.956
Case III	Stress (MPa)	11.23	12.173
	Deformation (mm)	0.00298	0.003017

VI. CONCLUSION

Results obtained for all the cases are closely matching with standard available results from MATLAB code. From these results we can conclude that model with inflatable material properties can be solved in ANSYS software. Small

variations in results are obtained because of use of simplified boundary conditions in ANSYS.

REFERENCES

1. Jeffrey D. Suhey(2005), Numerical Modeling and Design of Inflatable Structures- application to open-ocean- aquaculture cages, Elsevier, Aquacultural engineering.
2. The Effect of Flexibility on the Design and Performance of Inflatable Boats, plus Environmental Considerations P. Halswell – ph3e09@soton.ac.uk, P.A. Wilson, D.J. Taunton and S. Austen Nov 2013.
3. RichaVerma, Advancement in Inflatable –“A review”, International Journal of Engineering and Technology. ISSN 0974-3154 Volume 6, November 4 (2013), pp. 477-482.
4. Arbos-Torrent, S., Pang, Z. Y., Ganapathisubramani, B., Palacios, R., (2011) Leading and trailing edge effects on theaerodynamic performance of compliant aerofoils. In: 49th AIAA, No.1118, pp.1-16.
5. Bereznitski, A.,(2001) Slamming: The role of hydroelasticity. Int. shipbuilding progress 4, (48), pp. 333-351.
6. Bishop, R. E. D., Price, W. G.,(1979) Hydroelasticity of ships. Cambridge University Press.
7. Dand, I. W., (2002) Resistance measurements with an RNLI D-class Lifeboat. Report by BMT SeaTech; Doc No.3356.02.
8. Dand, I. W., Austen, S., Barnes, (2008)The speed of fast Inflatable Lifeboats. Int. Journal of Small Craft TechnologyVol. 150 Part B2, pp. 23-32.
9. Faltinsen, O. M.,(2005) Hydrodynamics of high-speed marine vehicles. Cambridge University Press, ISBN: 0-521-84568-8.
10. Gordnier, R.,(2009) High fidelity computational simulation of a membrane wing airfoil. Journal of Fluids and Structures25, (5), pp. 897-917.
11. Hirdaris, S. E., Temarel, P.,(2009) Hydroelasticity of ships: recent advances and future trends. Proceedings ofthe Institution of Mechanical Engineers, Part M: Journal of Engineering for the Maritime Environment 223, (3), pp. 305-330.
12. Savitsky, D., Morabito, M., (2010) Origin and characteristics of the spray patterns generated by planning hulls. Davidson Laboratory, Stevens institute of technology, Report No. 2882.
13. Townsend, N. C., Coe, T. E., Wilson, P. A., Shenoi, R. A.,(2010) On the mitigation of human motion exposure onboard high speed craft. Strategies and methods, includingflexible hull design. Private Communication.
14. L Puiga, A Bartonb, N Rando (2010), “A review on large deployable structures for astrophysics missions” ActaAstronautica, Volume 67, Issues 1– 2, July–August 2010, Pages 12–26.
15. S Voisembert, A Riwan, N Mechbal and A Barraco(2011),” A novel inflatable robot with constant and continuous volume”, Robotics and Automation (ICRA), 2011 IEEE International Conference on Digital Object Identifier, pp: 5843 – 5848